Stress relaxation and creep of cork

M. EMÍLIA ROSA, M. A. FORTES
Departamento de Engenharia de Materiais, Instituto Superior Técnico; Instituto de Ciência e Tecnologia dos Materiais, Av. Rovisco Pais, 1096 Lisboa Codex, Portugal

The stress relaxation and creep behaviour of cork under compression were characterized in tests done with the compression axis parallel to each of the three principal directions in the tree (radial, tangential and axial). All stress relaxations lead to a linear variation of stress with the logarithm of time, the slopes being nearly independent of stress and direction of compression. Creep stresses in the range 0.36 to 1.72 MPa were used. The strain rate continuously decreases during creep, from initial values around $10^{-4} \sec^{-1}$ to $\sim 10^{-7} \sec^{-1}$ after 8 h, but its dependence on the creep stress and direction of compression is not simple, mainly because different deformation regimes may operate during a single creep test. Compression loading–relaxation–unloading cycles were imposed on specimens, with compression either in the radial or in the tangential direction, with the purpose of simulating the performance of a cork stopper. A "work softening" is observed, i.e. the resistance decreases in successive compressions, particularly between the first two. This is explained in terms of an increased undulation of the cell walls produced in the first compression.

1. Introduction
In a previous paper [1] we reported on strain-rate effects on the room-temperature compression of cork, and on the recovery of dimensions upon unloading. It was concluded that the viscous component of deformation is quite important, with values of the strain rate sensitivity coefficient, $m = d(\ln \sigma)/d(\ln \dot{\varepsilon})$, around 0.06.

After unloading following compression, a cork sample partly or fully recovers its original dimensions, depending on the strain imposed. An empirical equation to describe the recovery as a function of time has been proposed [1], based on the experimental data.

The anisotropy of cork was clearly noted in these experiments, the radial direction being more resistant than the other two (tangential and axial), as already noted in previous studies of the mechanical properties of cork [2]. We found, however, clear evidence that the two non-radial directions, i.e. the axial and tangential directions, are not equivalent, the axial direction being slightly more resistant than the tangential direction, for most of the strain interval between 0 and 80%.

The scope of the present paper is complementary to that of the previous paper. Here we report on the stress relaxation and creep under compression of cork. We also describe the results of experiments aimed at simulating the load history experienced by a cork stopper, i.e. cycles of compression–relaxation–unloading (with recovery of dimensions). Cork stoppers have their axes parallel to a non-radial direction (usually the axial direction), because the pores (lenticular channels) in cork are parallel to the radial direction. The stress state in the stopper when it is in the bottle is of course biaxial, while all experiments were conducted in uniaxial compression. Nevertheless they show the main features of the behaviour of a

stopper, particularly what could be termed as the work-softening of cork, in the sense that a prior deformation reduces the stress required to produce a given strain. They also show why, in spite of the strong anisotropy of cork, a stopper retains its circular cross-section when removed from a bottle.

The stress relaxation can be described by simple equations, in contrast with what was found for the strain-rate effect and recovery of dimensions [1]. The creep behaviour is more complex and no simple correlations could be found between the strain rate and the creep stress. However, we have succeeded in rationalizing the experimental results in terms of the basic mechanisms of deformation of the cell walls in cork, as first described by Gibson *et al.* [2].

2. Experimental procedure
The cork used in most of the experiments was of the same batch previously used in the study of strain-rate effects and recovery of dimensions [1]. It is a good-quality cork, and was previously submitted to a boiling operation. The number of cells per unit volume is $\sim 6 \times 10^7 \, cm^{-3}$ and the cell wall thickness is $\sim 1.5 \, \mu m$. The density is $172 \pm 6 \, kg \, m^{-3}$.

In some of the stress relaxation experiments another batch of (boiled) cork was used, of density $128 \, kg \, m^{-3}$. The lower density is associated with larger cell dimensions and not with a larger pore volume or a smaller cell wall thickness.

As previously, the specimens were in the form of cubes with their edges parallel to the three principal directions in cork, which were identified in the specimens. The cube edge was 16 mm in the creep tests and 20 mm in the other tests. All tests were conducted at room temperature, with the cork specimens equilibrated in the ambient atmosphere

(water content, measured by weight loss at $100°C$, of 7%).

The stress relaxations were done during compression tests at constant crosshead speed. The crosshead was stopped at pre-chosen strains and a load against time curve was recorded. The creep tests were done in the same tensile machine, following compression to the creep stress at a load rate of $5 N sec^{-1}$. Four creep stresses were used. The displacement of the crosshead was monitored as a function of time, in each experiment. From this, the strain and strain rate were obtained. The strain is defined as $(L_0 - L)/L_0$, where L_0 is the initial dimension and L is the current dimension. Each of the four creep stresses was applied in different specimens, along each of the three principal directions. Three specimens were tested for each combination. The tests lasted for 8 h each.

In the experiments aimed at simulating a cork stopper, the specimens were compressed to a given strain (30%) and allowed to stress-relax for 10 min. The specimens were then unloaded and left in this condition for 10 min. Finally, they were compressed again to the same strain, relaxed and unloaded for the same time intervals, and so forth. Ten such cycles were imposed, both in the radial and in the tangential direction.

3. Results

3.1. Stress relaxation

The stress relaxation tests of the low-density cork were done during compression tests at $\dot{\varepsilon} = 8.3 \times 10^{-3} sec^{-1}$.* The axis of compression was either radial or perpendicular to the radial direction, with no identification of this latter direction. For each specimen, stress relaxations were done successively for strain values corresponding to each of the three regions that can be identified in the compression curves. For example, for the radial direction the strains during relaxation were 5.7, 30 and 67%, each corresponding to a different region of the compression curve. Each of these regions corresponds to a different deformation mechanism [1, 2], respectively, cell wall bending, post-buckling deformation, and deformation of collapsed walls, with mutual contacts (cell wall crushing).
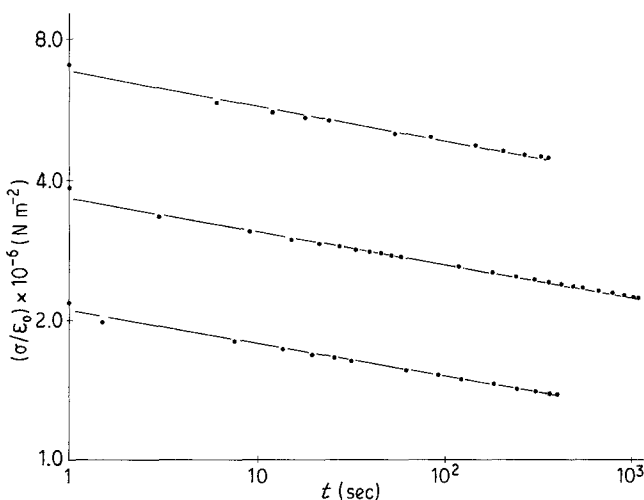
The stress (nominal stress) divided by the strain during relaxation, ε_0, was plotted as a function of time in log–log scales. Fig. 1 shows results for the radial direction. The relaxation data for the non-radial direction also gave straight lines with nearly the same slopes. Indeed, the same linear relation was found in all relaxations done in the higher-density cork, as will be described below.

The stress relaxation of cork can then be described by a simple power law

$$\frac{\sigma}{\varepsilon_0} = kt^{-\alpha} \qquad (1)$$

The values of α ranged from 0.065 to 0.075 for the lighter cork and from 0.045 to 0.060 for the denser cork. The value of k decreases as ε_0 increases. For the curves of Fig. 1, k decreases from 6.77×10^6 to 3.64×10^6 (SI units). Slightly larger values of k were obtained with the higher-density cork.

3.2. Compression–relaxation–unloading cycles

More stress relaxation data were obtained in the experiments aimed at simulating the stress cycles to which a cork stopper is submitted when it is successively introduced and removed from a wine bottle. The cork used in these experiments was of the higher-density batch ($\varrho = 172 kg m^{-3}$). The compression was carried out up to $\varepsilon = 30\%$ in the radial and in the tangential directions in different experiments (three for each direction), at a crosshead speed of $2 mm min^{-1}$ ($\dot{\varepsilon} = 1.7 \times 10^{-3} sec^{-1}$). The relaxations that followed lasted for 10 min, after which the specimens were unloaded at a crosshead speed of $500 mm min^{-1}$ and left for 10 min in the unloaded condition. This cycle was repeated ten times. The strain recovered during unloading was measured by the displacement of the machine crosshead.

Fig. 2 shows the strain history of one particular specimen, compressed in the radial direction. It is noted that the length parallel to the compressed direction does not fully recover during the 10 min unloading, which is consistent with the results previously reported [1]. Fig. 3 contains five selected compression

Figure 1 Stress relaxation curves obtained with the lower-density cork, after compression in the radial direction to increasing strains, respectively, from top to bottom: 5.7%; 67%; 30%. Log–log scales. The points on the σ/ε_0 axis correspond to the beginning of relaxation ($t = 0$).

*The strain rate, $\dot{\varepsilon}$, is defined as the ratio of the crosshead speed to the initial length parallel to the compression axis. It is $\dot{\varepsilon} = \dot{L}/L_0$.

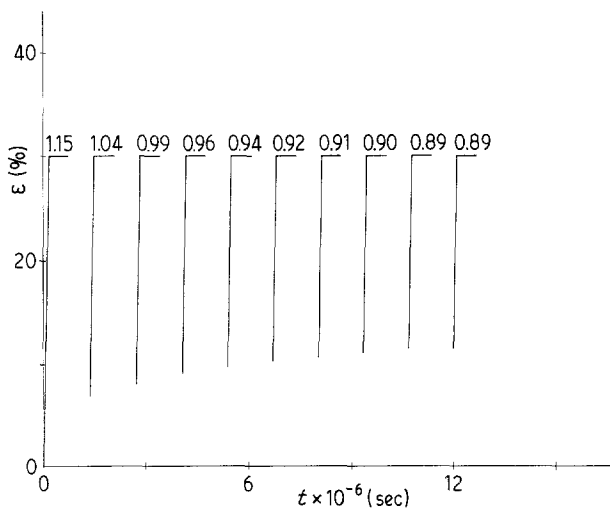Figure 2 The strain, ε, as a function of time, t, in the compression cycle experiments in the radial direction. The large-slope regions of the curves are for the compression part of cycles, the horizontal segments correspond to the stress relaxations and the gaps between curves to the unloadings. The figures on each curve are the stresses, in MPa, at the end of each compression.

Figure 4 Successive stress–strain curves in a compression-cycle experiment (tangential compression). Ten cycles were applied but the compression curves are shown only for the 1st, 2nd, 4th, 8th and 10th compression, in the order (left to right) of increasing strain for $\sigma = 0$.

curves $\sigma(\varepsilon)$ in the ten compression cycles of the specimen of Fig. 2 (compression in the radial direction): the curves included are for the 1st, 2nd, 4th, 8th and 10th compressions. Note that the permanent deformation at the beginning of compression increases in successive cycles. Fig. 4 contains data of the same type as Fig. 3 but for compression in the tangential direction. The curves of Figs 3 and 4 (and also of Fig. 2) are for a particular specimen. The curves for the other two specimens tested in each direction are similar, but the usual scatter was found in the position of the corresponding curves (see the standard deviations in Tables I and II below).

A Young's modulus was determined in each loading part of the cycles from the average slope between length changes of 0.2 and 0.3 mm relative to the initial length at the beginning of compression. The values of the modulus are indicated in Table I. For example, for the specimen to which Figs 2 and 3 refer (radial compression), the measured modulus decreases from 11.1 to 6.1 MPa, the decrease being almost entirely accomplished in the second cycle.

A remarkable characteristic of the compression curves of Figs 3 and 4 is as follows. The first compression curve clearly shows the transition associated with the start of cell wall buckling, which separates the
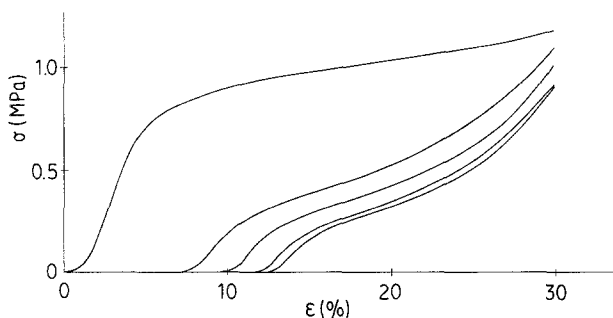
first two regions of the curve [1–3]. This transition is much less sharp in subsequent curves, which have nearly the same shape, although a slight decrease both in the initial slope (Young's modulus, see Table I) and in the buckling stress can be observed in successive curves from the 2nd to the 10th. No tests were done for compression in the axial direction. It is known [1, 2] that this direction behaves approximately in the same way as the tangential direction.

Table II shows the evolution of other quantities measured in successive cycles of compression in the radial and in the tangential directions. Average values for the three specimens tested for each direction are indicated, together with the standard deviations. The values shown in Table II are the strain, ε_i, at the beginning of a compression, the stress, σ_{30}, at the final strain of 30% and the stress, σ_f, at the end of the 10 min relaxation. It is noticeable that the stresses σ_{30} and σ_f remain appreciably larger for the radial direction in successive cycles (dashed lines in Fig. 5). This suggests that the stress state in a cork stopper inserted in a bottle is not symmetrical about the axis of the stopper.

In Fig. 5 is plotted the stress, σ_{30}, required to produce the strain $\varepsilon = 30\%$ in successive compressions, as a function of the strain at the beginning of the compressions. The curves are average curves for the three specimens tested in each case. The tangential direction is less resistant than the radial direction, as already pointed out [1]. The ratio of the σ_{30} in the first and final compressions is ~ 1.3 both for the radial and tangential directions.

The stress relaxation results for the successive

Figure 3 Successive stress–strain curves in a compression cycle experiment (radial compression). Ten cycles (see Fig. 2) were applied but the curves are shown only for the 1st, 2nd, 4th, 8th and 10th compressions, in the order (left to right) of increasing strain for $\sigma = 0$.
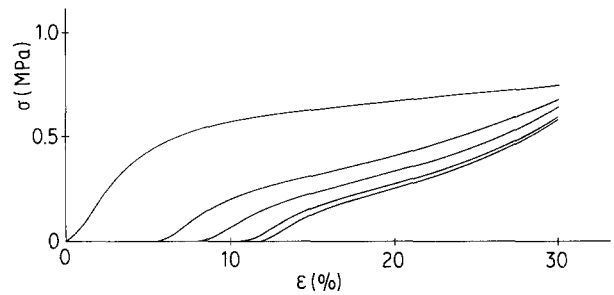
TABLE I Young's modulus in successive compressions

Compression	E (MPa)	
	Radial	Tangential
1st	11.1 ± 4.5	8.2 ± 3.7
2nd	6.7 ± 2.0	4.0 ± 1.2
3rd	6.8 ± 1.8	3.9 ± 1.5
4th	6.5 ± 1.2	3.7 ± 1.3
5th	6.3 ± 1.2	3.4 ± 1.4
6th	6.1 ± 1.9	3.1 ± 1.0
7th	6.2 ± 1.3	3.1 ± 1.0
8th	5.9 ± 1.6	3.0 ± 1.2
9th	6.0 ± 1.2	3.1 ± 1.3
10th	6.1 ± 1.3	2.8 ± 1.0

37

TABLE II Data from compression-cycle experiments*

Cycle No.	Radial			Tangential		
	ε_i (%)	σ_{30} (MPa)	σ_f (MPa)	ε_i (%)	σ_{30} (MPa)	σ_f (MPa)
1	0	1.15 ± 0.06	0.77 ± 0.03	0	0.79 ± 0.05	0.55 ± 0.04
2	6.8 ± 0.5	1.04 ± 0.05	0.73 ± 0.03	5.9 ± 0.5	0.73 ± 0.05	0.53 ± 0.04
3	8.0 ± 0.3	0.99 ± 0.05	0.70 ± 0.03	7.3 ± 0.5	0.72 ± 0.06	0.52 ± 0.04
4	9.1 ± 0.4	0.96 ± 0.05	0.69 ± 0.04	8.6 ± 0.4	0.66 ± 0.05	0.49 ± 0.04
5	9.7 ± 0.6	0.94 ± 0.05	0.68 ± 0.03	9.3 ± 0.4	0.65 ± 0.05	0.48 ± 0.04
6	10.2 ± 0.6	0.92 ± 0.05	0.67 ± 0.03	9.8 ± 0.4	0.65 ± 0.05	0.48 ± 0.04
7	10.6 ± 0.7	0.91 ± 0.05	0.66 ± 0.03	10.3 ± 0.4	0.63 ± 0.05	0.47 ± 0.04
8	11.0 ± 0.6	0.90 ± 0.05	0.65 ± 0.03	10.7 ± 0.3	0.63 ± 0.06	0.47 ± 0.04
8	11.4 ± 0.7	0.89 ± 0.05	0.65 ± 0.03	11.1 ± 0.2	0.63 ± 0.06	0.47 ± 0.05
10	11.5 ± 0.7	0.89 ± 0.05	0.65 ± 0.03	11.5 ± 0.1	0.62 ± 0.05	0.46 ± 0.04

*ε_i = accumulated strain at beginning of cycle; σ_{30} = stress at ε = 30%; σ_f = stress at end of 10 min relaxation.

relaxations are plotted in Figs 6a and b for the radial and tangential directions of compression, respectively. The dependence of log σ on log t is linear, as also found for the lower-density cork, with slopes α (see Equation 1) nearly independent of the initial strain and direction of compression. The values of α ranged from 0.045 to 0.060 and are slightly smaller than those obtained for the lighter cork.

Finally, the recovery of length (parallel to the compression axis) in the 10 min unloading following the successive compressions is shown in Fig. 7 as a function of the stress σ_{30}, for the radial and tangential directions. The recovered strains in the two directions become nearly equal after the first four to six cycles (dashed lines in Fig. 7), which may explain why a cork stopper removed from a bottle does not tend to ovalize.

3.3. Creep tests
Creep tests were done with the higher-density cork (ϱ = 172 kgm^{-3}) compressed in each of the three principal directions. Four stresses were used: 0.36,

Figure 5 The stress, σ_{30}, required to produce the strain ε = 30% as a function of strain at the beginning of successive compressions in the compression cycle experiments. R = radial compression; T = tangential compression. Each dashed line defines points (e.g. P, P') corresponding to the same number of order of the cycle: 2nd, 4th, 8th and 10th from left to right.

0.55, 0.77 and 1.72 MPa. The first is in the elastic region for all directions (see stress–strain curves in the previous paper [1]). The stress of 0.77 MPa is in the plateau region for all directions, but 0.55 MPa is in the first region for the radial direction and in the second region for the non-radial directions. Finally, the larger stress, 1.72 MPa, is near the end of the plateau region, and more so for the non-radial directions.

Each creep experiment lasted for 8 h. The strain was automatically recorded every 1 min for the first 30 min and then every 5 to 10 min. Three tests were done for each stress and for each direction of compression.

The full creep curves $\varepsilon(t)$ are shown in Figs. 8a to d. Each figure refers to a particular stress and contains average creep curves for each of the three directions.

The slope of the curves continuously decreases as shown in examples in Fig. 9: a steady-state creep stage does not occur. This is more clearly seen in Fig. 10, where the strain rate $\dot{\varepsilon}$ is plotted as a function of ε, with ε defined in relation to the unloaded length. The strain at the beginning of the creep test is the strain produced in loading to the creep stress. The strain rate continuously decreases during the tests, from initial values, $\dot{\varepsilon}_0$, around 10^{-4} sec^{-1} to final values, $\dot{\varepsilon}_f$, (8 h) of $\sim 10^{-7}$ sec^{-1}.

The different shapes and slopes of the creep curves indicate that creep of cork is a complex phenomenon, making hopeless the search for simple rate equations that may describe it. This is in contrast with the simple behaviour in stress relaxation, and may be due to the fact that, under creep, different deformation mechanisms are operating. This will be discussed further in the final section.

More data on the creep behaviour of cork are given in Table III, which helps in comparing the various directions in which the creep load was applied. The table indicates the initial and final strains and strain rates for each direction of the four creep stresses used in the experiments.

From Figs 8 to 10 and the data of Table III the following conclusions can be drawn. The radial direction is more creep-resistant than the non-radial directions. Among these, the axial direction is slightly more resistant than the tangential direction, a difference also found in the compression tests described in the previous paper [1]. These conclusions are based on the comparison of the strains measured at the end of creep (Table III, 4th column). If we consider the strains
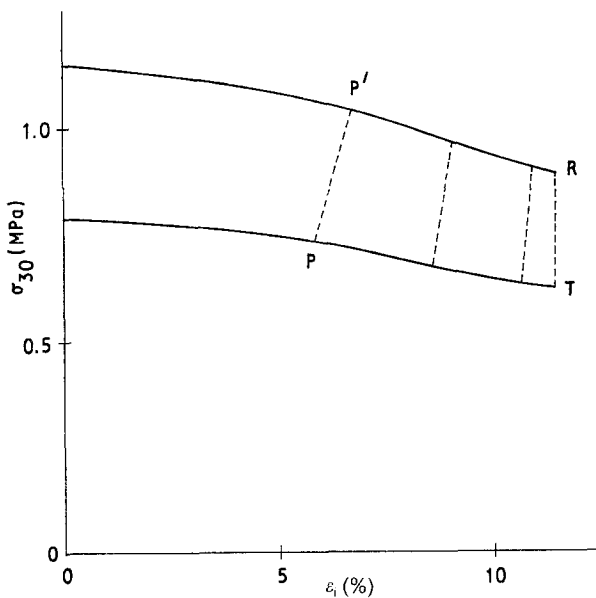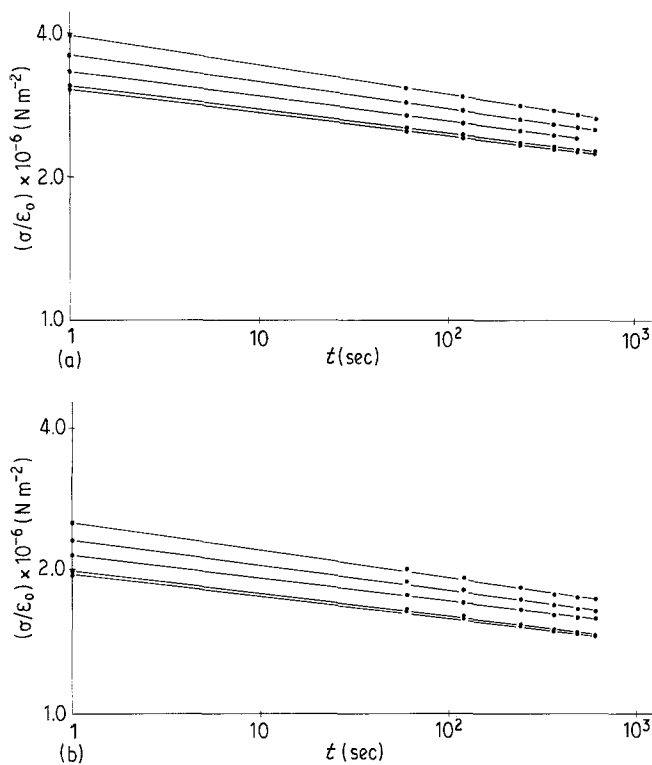
Figure 6 Stress relaxation curves following successive compressions of the higher-density cork: (a) in the radial direction; (b) in the tangential direction. The curves correspond, from top to bottom, to the 1st, 2nd, 4th, 8th and 10th relaxations in the compression-cycle experiments. Log–log scales. The points on the σ/ε_0 axis correspond to the beginning of relaxation ($t = 0$).

produced exclusively during creep (Table III, 5th column) we find that they increase in the order radial–axial–tangential direction for the three lower creep stresses, but for the larger creep stress the order is reversed. This does not invalidate the conclusion drawn above on the relative deformation resistance of the different directions. The reason why the radial direction seems to be weaker under this criterion is merely due to the fact that this high stress corresponds to the final stage of deformation (cell wall crushing) for the non-radial directions, but to the second, cell-wall buckling stage, for the radial direction.

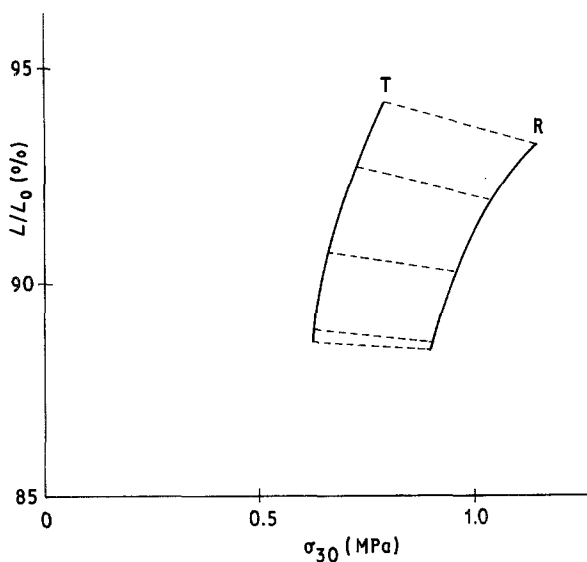The same inversion is also observed in the values of

Figure 7 Recovery of the length of the edge parallel to the direction of compression in successive unloading periods of the compression-cycle experiments. The recovery is defined as L/L_0 where L is the length after the 10 min recovery, and is plotted as a function of the stress σ_{30} at the end of successive compressions. R = radial compression, T = tangential compression. The dashed lines have the meaning explained in the caption of Fig. 5 and correspond to the following cycles: 1st, 2nd, 4th, 8th and 10th, from top to bottom.

the strain rate at the beginning and end of creep, the increasing order of which for the three directions is radial–axial–tangential for the lower stresses, but not for the larger stress. Even the effect of stress on the creep strain rate shows this anomaly: the strain rate at the beginning of creep and, more clearly, the strain rate after 8 h, do not increase as the creep stress increases from 0.77 to 1.72 MPa.

4. Discussion

The stress relaxation of cork is very well described by a linear relation between $\log (\sigma/\varepsilon_0)$ and $\log t$ (Equation 1). The slope, $-\alpha$, of the lines is isotropic and approximately independent of the strain ε_0 during relaxation, but seems to be affected by the density of cork, with a smaller α for the denser cork. This behaviour suggests that the viscous stress relaxation of the cell walls is due to the same mechanisms, independent of the overall strain imposed on cork.

When cork is successively compressed, relaxed and unloaded, as with a cork stopper, a softening, or decrease of resistance, is observed, in the sense that the stress required to produce a given final strain (i.e. a given final dimension parallel to the direction of compression) decreases as successive compression–relaxation–unloading cycles are imposed. The stress probably tends to a constant value, but this was not reached after the ten cycles used in the experiments. During the 10 min period of unloading the strain is partly recovered. The recovered strain probably also tends to a constant value, as the data seem to indicate.

We shall now attempt a semi-quantitative explanation of the results obtained in the compression-cycle experiments, based on the accepted ideas on the mechanisms of deformation of cork, and on the fact that the prismatic cells in cork have their lateral faces corrugated. At low strains, the cell walls bend. In the theory of Gibson *et al.* [2, 3] of cellular materials, the cell walls are modelled by thin planar plates of thickness
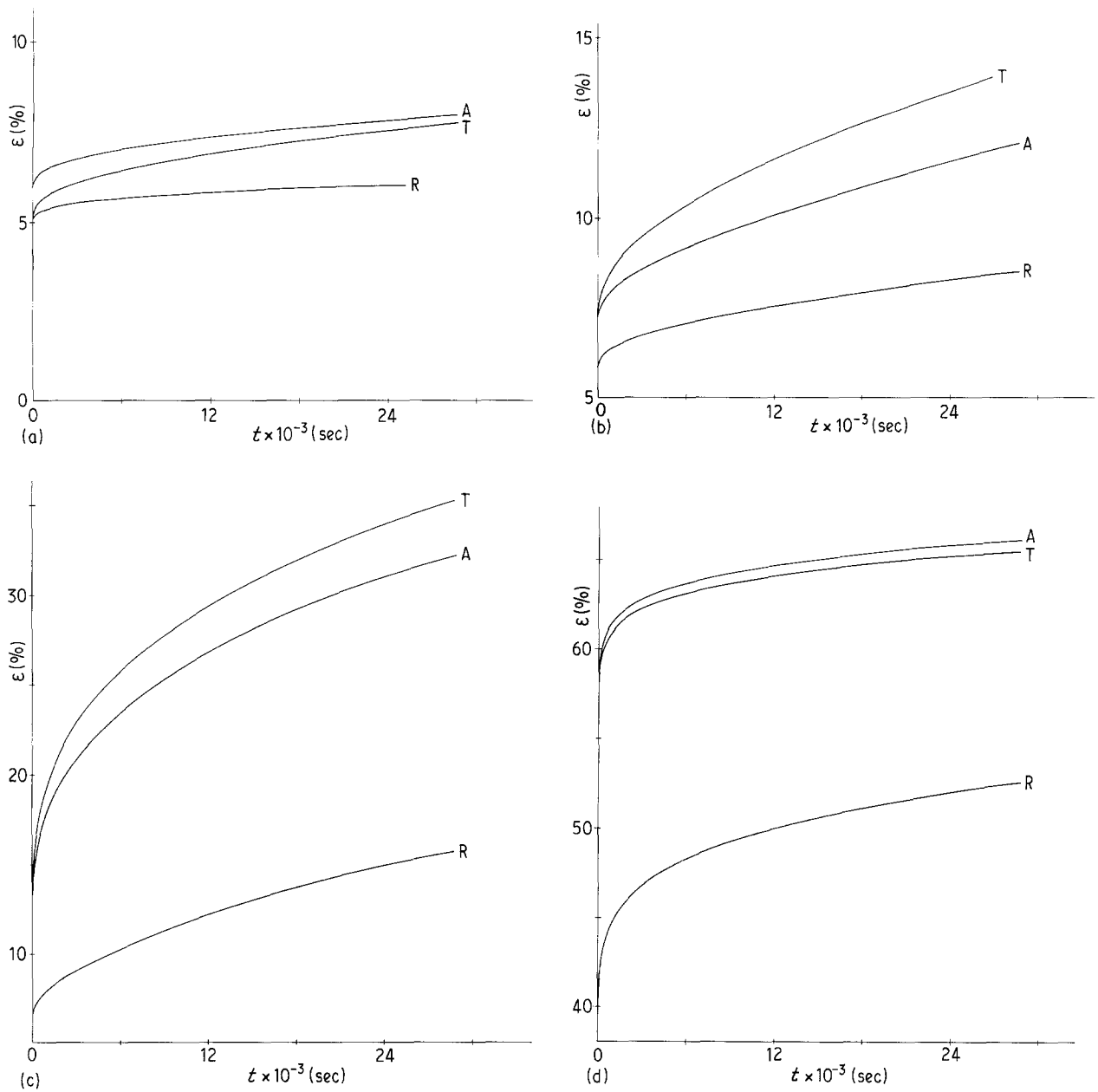
Figure 8 Creep curves for cork compressed in each of the principal directions: R = radial, T = tangential, A = axial. The creep stresses are: (a) 0.36 MPa, (b) 0.55 MPa, (c) 0.77 MPa, (d) 1.72 MPa.

TABLE III Data from creep tests at various compression stresses applied in each principal direction of cork*

Creep stress (MPa)	Direction of compression	ε_0 (%)	ε_f (%)	$\Delta\varepsilon$ (%)	$\dot{\varepsilon}_0$ (sec^{-1})	$\dot{\varepsilon}_f$ (sec^{-1})
0.36	Radial	5.1 ± 1.1	6.1 ± 1.2	1.0 ± 0.1	$(1.1 \pm 0.4) \times 10^{-5}$	$(2.1 \pm 0) \times 10^{-7}$
	Axial	6.0 ± 0.3	8.0 ± 0.5	2.0 ± 0.2	$(2.2 \pm 1.3) \times 10^{-5}$	$(2.8 \pm 1.2) \times 10^{-7}$
	Tangential	5.0 ± 0.7	7.8 ± 0.6	2.8 ± 0.1	$(3.4 \pm 1.0) \times 10^{-5}$	$(3.8 \pm 2.4) \times 10^{-7}$
0.55	Radial	5.8 ± 1.0	8.5 ± 1.4	2.7 ± 0.4	$(2.0 \pm 0.3) \times 10^{-5}$	$(5.6 \pm 0.6) \times 10^{-7}$
	Axial	7.1 ± 0.2	12.1 ± 0.8	5.0 ± 0.6	$(2.7 \pm 0.3) \times 10^{-5}$	$(1.1 \pm 0.3) \times 10^{-6}$
	Tangential	7.2 ± 1.0	14.9 ± 4.8	7.7 ± 3.8	$(4.4 \pm 2.0) \times 10^{-5}$	$(1.5 \pm 0.8) \times 10^{-6}$
0.77	Radial	6.6 ± 0.4	15.7 ± 3.1	9.1 ± 2.7	$(4.5 \pm 0.7) \times 10^{-5}$	$(1.5 \pm 0.3) \times 10^{-6}$
	Axial	11.6 ± 1.6	32.1 ± 9.1	20.5 ± 7.5	$(2.9 \pm 2.1) \times 10^{-4}$	$(2.1 \pm 0.2) \times 10^{-6}$
	Tangential	11.3 ± 1.6	35.1 ± 3.3	23.8 ± 1.7	$(3.7 \pm 0.8) \times 10^{-4}$	$(2.5 \pm 0.4) \times 10^{-6}$
1.72	Radial	39.3 ± 1.1	52.5 ± 2.0	13.2 ± 0.9	$(2.6 \pm 0.7) \times 10^{-4}$	$(1.1 \pm 0.4) \times 10^{-6}$
	Axial	56.5 ± 7.1	66.0 ± 4.3	9.5 ± 2.8	$(3.3 \pm 1.7) \times 10^{-4}$	$(6.2 \pm 0.1) \times 10^{-7}$
	Tangential	57.7 ± 0.9	65.4 ± 1.5	7.7 ± 0.6	$(1.4 \pm 0) \times 10^{-4}$	$(5.8 \pm 0.9) \times 10^{-7}$

*ε_0, ε_f = strains at beginning/end of creep test; $\Delta\varepsilon = \varepsilon_f - \varepsilon_0$; $\dot{\varepsilon}_0$, $\dot{\varepsilon}_f$ = strain rates at beginning/end of creep test.
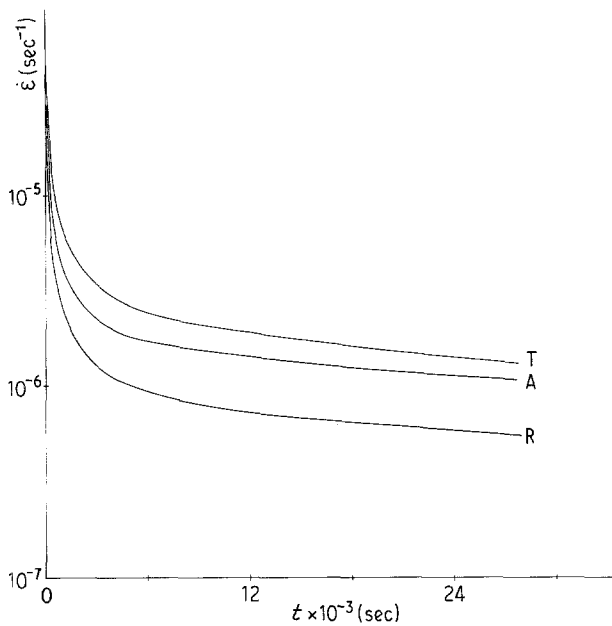
Figure 9 The strain rate as a func-
tion of time in a creep test under
a stress of 0.55 MPa applied par-

allel to each principal direction:
R = radial, T = tangential,
A = axial.

t, Young's modulus E_w and density ϱ_w. For com-
pression in the radial direction the model predicts a
Young's modulus E given by

$$E \simeq 0.7 E_w \frac{\varrho}{\varrho_w} \tag{2}$$

where ϱ is the (macroscopic) density of the material.
The stiffness of a corrugated plate with sinusoidal
undulations of amplitude a is smaller than that of a
planar plate of the same material and thickness. The
effective Young's modulus, E_w, is related to the
Young's modulus of the cell wall material, E_s, by [2]

$$E_w = E_s \left(1 + \frac{6a^2}{t^2} \right)^{-1} \tag{3}$$
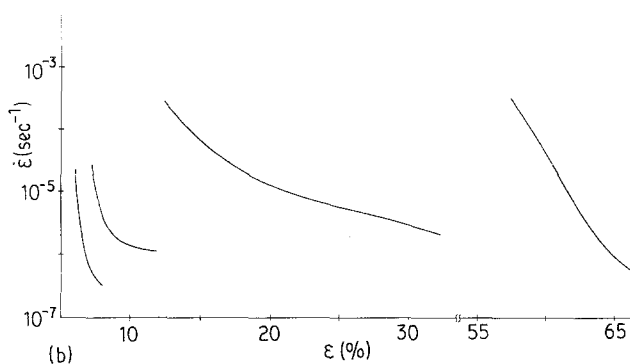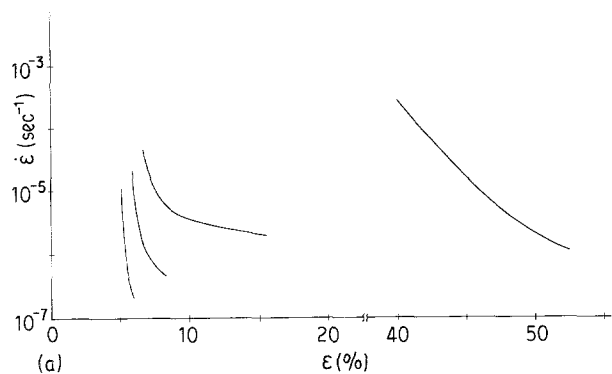
where t is the thickness. It is difficult with these
equations to predict the absolute values of the
Young's modulus because E_w and ϱ_w are not known
with sufficient accuracy, but they can be more accur-
ately used to study the effect of the amplitude of the
undulations on the modulus.

In the first compression of 30%, the cell walls
buckle and become more corrugated. The geometry of
the corrugations is not altered during relaxation
because the strain is kept constant, but the stress
decreases due to viscous phenomena which occur in
the cell walls. When the stress is removed, the cell walls
tend to straighten, but remain more corrugated than
they were initially, since the recovery is only partial.
Their E_w is therefore smaller than initially. Using the
measured values of the Young's moduli of the 1st and
2nd compression, and assuming that initially $a = 2t$,
we obtain for the amplitude a at the beginning of the
2nd compression a value of $2.6t$. This means that the
average amplitude of the undulations increased by
30% in the buckling during the first compression,
which seems reasonable. In the compressions follow-
ing the first, the cell walls had already buckled and
probably do not suffer additional buckling. This
explains the shape of the corresponding compression
curves, which do not exhibit the sharp transition due
to buckling, observed in the first curve. The slight
decrease in the Young's modulus measured in these
curves can be due to the decrease in the recovered
strain, which implies that the amplitude of corru-
gations at the beginning of compression slightly
increases in successive compressions.

As already pointed out, the complexity of the creep
behaviour of cork is in part due to the fact that dif-
ferent deformation mechanisms (bending of walls,
buckling of walls, crushing of walls) can occur during
a single creep experiment. The initial strain rate in a
creep test always increases as the stress increases, and
shows the anisotropy expected from the relative resist-
ance to compression of the radial, tangential and axial
directions. The strain rate decreases during creep, but
even after 8 h at room temperature it has an appreci-
able value ($\dot{\varepsilon} \simeq 10^{-7} \sec^{-1}$). The values of the creep
rate after 8 h, for a given stress, are not in the expected
sequence for the three directions when different

Figure 10 The strain rate, $\dot{\varepsilon}$, in creep, as a function of the accumu-
lated strain, ε ($\varepsilon = 0$ corresponds to the unloaded specimens) for
the four stresses used in the experiments: 0.36, 0.55, 0.77 and
1.72 MPa, from left to right. (a) Creep in the radial direction, (b) in
the axial direction, (c) in the tangential direction.
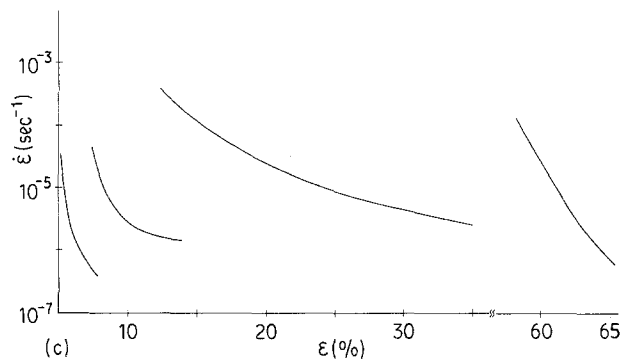
deformation mechanisms are in operation for the different directions. This is particularly noticeable at the higher stress used, which is, in terms of the "crushing of walls" regime, a larger stress for the non-radial directions. The crushing of walls is expected to be a slower process than the post-buckling bending of walls, which explains why a lower strain rate is observed at long times in the non-radial directions, under the higher stress.

The creep data shown in Figs 8 to 10 are difficult to extrapolate to other stresses and, more so, to larger times. A cork specimen under a small creep stress may even show the three deformation regimes, provided that the (small) stress is applied for a sufficiently long time. The data obtained in the creep experiments described in this paper must then be regarded as an order-of-magnitude indication of the creep strain rates that can be produced. It is also expected that large variations in creep rate will be found between specimens of different batches of cork, the creep rate probably increasing as the density decreases, except, perhaps, when the crushing-of-walls regime is reached, in which case the creep rate should be fairly independent of density.

References

1. M. EMÍLIA ROSA and M. A. FORTES, *J. Mater. Sci.* **22** (1987) 000.
2. L. J. GIBSON, K. E. EASTERLING and M. F. ASHBY, *Proc. R. Soc.* **A377** (1981) 99.
3. M. F. ASHBY, *Met. Trans.* **14A** (1983) 1755.